



Article

Adaptive Dynamic Surface Control of Strict-Feedback Fractional-Order Nonlinear Systems with Input Quantization and External Disturbances

Fan Zhang ¹, Xiongfeng Deng ^{2,*} and Lisheng Wei ²

¹ Key Laboratory of Advanced Perception and Intelligent Control of High-End Equipment, Ministry of Education, Anhui Polytechnic University, Wuhu 241000, China

² Key Laboratory of Electric Drive and Control of Anhui Higher Education Institutes, Anhui Polytechnic University, Wuhu 241000, China

* Correspondence: dengxiongfeng@ahpu.edu.cn

Abstract: In this work, an adaptive dynamic surface control law for a type of strict-feedback fractional-order nonlinear system is proposed. The considered system contained input quantization and unknown external disturbances. The virtual control law is presented by utilizing a dynamic surface control approach at each step, where the nonlinear compensating term with the estimation of unknown bounded parameters is introduced to overcome the influence of unknown external disturbances and surface errors. Meanwhile, the adaptive laws of relevant parameters are also designed. In addition, an improved fractional-order nonlinear filter is developed to deal with the explosion of complexity raised by the recursive process. In the last step, an adaptive dynamic surface control law is proposed to ensure the convergence of tracking error, in which the Nussbaum gain function is applied to solve the problem of the unknown control gain generated by input quantization. Then, the fractional Lyapunov stability theory is applied to verify the stability of the proposed control law. Finally, simulation examples are given to illustrate the effectiveness of the proposed control law.

Keywords: strict-feedback fractional-order systems; fuzzy logic system; dynamic surface control; input quantization



Citation: Zhang, F.; Deng, X.; Wei, L. Adaptive Dynamic Surface Control of Strict-Feedback Fractional-Order Nonlinear Systems with Input Quantization and External Disturbances. *Fractal Fract.* **2022**, *6*, 698. <https://doi.org/10.3390/fractalfract6120698>

Academic Editor: Ravi P. Agarwal

Received: 6 October 2022

Accepted: 19 November 2022

Published: 25 November 2022

Publisher's Note: MDPI stays neutral with regard to jurisdictional claims in published maps and institutional affiliations.



Copyright: © 2022 by the authors. Licensee MDPI, Basel, Switzerland. This article is an open access article distributed under the terms and conditions of the Creative Commons Attribution (CC BY) license (<https://creativecommons.org/licenses/by/4.0/>).

1. Introduction

In the past several decades, fractional calculus has received tremendous attention because many complex physical phenomena can be characterized by fractional-order systems [1–5]. Many distinguished results related to stability analysis and control schemes have been reported [6–9]. In addition, many fractional-order control approaches, such as fractional-order terminal sliding mode control [10], fractional-order prescribed performance control [11], fractional-order fuzzy control [12,13], fractional-order neural network control [14], fractional-order neuro-fuzzy control [15], have been designed and applied through the combination of fractional-order operators and classical control methods. However, it should be emphasized that, in many cases, the control methods of integer-order systems cannot be directly extended to fractional-order systems. Therefore, the control of fractional-order systems is still a problem with both great potential and challenges, which inspires this work.

It is widely known that, as an efficient control tool, backstepping control establishes a system framework for the control design of nonlinear systems. In this method, the studied system is decomposed into several subsystems, and a virtual control law is designed for each step until the actual control law is obtained, which greatly reduces the design of the control law. To date, various results have been presented for integer-order systems with backstepping control [16–19]. Unfortunately, for the noninteger-order systems with backstepping control, only a few research efforts have been made. For example, in [20], an

adaptive neural network backstepping control scheme was proposed for fractional-order nonlinear systems with actuator faults, in which the neural network was introduced into the recursive design to approximate the unknown nonlinear dynamics. In [21], the authors addressed an adaptive backstepping hybrid fuzzy sliding mode control method and solved the finite-time tracking control problem of a type of uncertain fractional-order nonlinear system. In [22], an adaptive backstepping control scheme was developed for a type of fractional-order nonlinear system, in which the external disturbance and uncertain parameters were considered, and an auxiliary function was designed to replace the discontinuous function (such as the sign function) to obtain a smooth control input. It should be pointed out that there is an obvious problem with the results mentioned above, that is, the complexity explosion problem caused by repeated differentiation in the recursive design of backstepping controls. How to avoid this issue to achieve the stability of backstepping for fractional-order systems is a hot topic, which is another inspiration of this work.

For one thing, to overcome the explosion of complexity in recursive design, some researchers have applied the dynamic surface control approach, or the command filtered control technique, to simplify the design process [23–26]. Based on the application of first-order or second-order filters, the repeated differentiation in recursive design is skillfully avoided. Up to now, many excellent results have been produced in the control of fractional-order systems. In [27,28], a control law for uncertain fractional-order nonlinear systems was designed by applying the backstepping dynamic control technique, where the unknown external disturbance and the approximation error were compensated using a designed auxiliary function. In [29], a compound learning adaptive dynamic surface control method was proposed for fractional-order nonlinear systems, which guarantees that the tracking error can converge. In [30,31], the neural network command filtering control of fractional-order systems with actuator faults was addressed, in which the control problems of finite-time control and synchronization control were solved using the proposed control schemes. As far as we know, the adaptive dynamic surface control of fractional-order nonlinear systems has not been fully developed in the existing literature, especially in the case of the strict-feedback form.

In addition, the performance of a system may degrade due to external factors (for example, input saturation, external disturbances and limited bandwidth) or even as a result of damage to the stability of the system. Therefore, it is worth devoting attention to the design of a suitable controller to reduce the effects of external factors in the system. Considering the existence of input saturation, external disturbance and input quantization, some related results, such as the barrier function-based adaptive sliding mode control law, the observer-based control law and the command filter-based adaptive fixed-time control law, have been obtained by studying integer-order systems and fractional-order systems [32–35]. However, these external factors may also lead to an unknown control direction of the system. To solve the control problem of unknown control direction, some researchers introduced the Nussbaum control technique [36,37]. For fractional-order nonlinear systems, the problem of unknown control direction is a topic worthy of attention, but there are few research results in this area.

Motivated by the above discussion, this work addresses the control problem of adaptive dynamic surface control for strict-feedback fractional-order nonlinear systems with input quantization and unknown external disturbances. The main contributions can be summarized as follows:

(i) An adaptive dynamic surface control law was developed for the strict-feedback fractional-order nonlinear systems with input quantization and external disturbances. Different from [12,15,22], the unknown parameters, unknown external disturbances and unknown control direction were considered simultaneously, and an improved fractional-order nonlinear filter with an adaptive law was introduced to solve the explosion of complexity problem created by repeatedly differentiating the virtual control law.

(ii) To overcome the influence of unknown external disturbances and surface errors, nonlinear auxiliary functions with the estimation of unknown bounded parameters were introduced into the design of virtual control laws and the final actual control law. This differed from the results of [38,39].

(iii) To solve the problem of the unknown control gain raised by input quantization, the Nussbaum gain function technique was considered in the design of the actual control law. Compared with references [34,35], the final control law design in this paper was simplified.

The rest of this paper is organized as follows: Preliminaries and the problem formulation are provided in Section 2. In Section 3, the design of the adaptive dynamic surface control law is shown in detail, and then the stability analysis is outlined. The simulation environment and methods are given in Section 4 to illustrate the effectiveness of the proposed control law, and the results and discussion are presented in Section 5. Finally, some brief conclusions to this paper are given in Section 6.

2. Preliminaries and Problem Formulation

2.1. Preliminaries

First, some basic definitions and lemmas of fractional calculus are provided.

Definition 1 [27]. Assuming that $h(t) : [t_0, +\infty) \rightarrow R$ is a continuously differentiable function, its Caputo fractional-order derivative with order α is defined as

$${}^c\mathcal{D}_t^\alpha h(t) = \frac{1}{\Gamma(1-\alpha)} \int_{t_0}^t (t-s)^{-\alpha} h'(s) ds \tag{1}$$

where $\alpha \in (0, 1)$ and ${}^c\mathcal{D}_t^\alpha$ stands for the Caputo fractional-order differential operator with order α , and $\Gamma(\Delta) = \int_0^{+\infty} s^{\Delta-1} e^{-s} ds$. Here, $\Gamma(\cdot)$ stands for the gamma function and satisfies $\Gamma(1) = 1$.

Definition 2 [7]. The two-parameter Mittag-Leffler function is described as

$$E_{\alpha,\beta}(z) = \sum_{j=0}^{\infty} \frac{z^j}{\Gamma(j\alpha + \beta)} \tag{2}$$

where $\alpha, \beta > 0$ are constants and $z \in \mathbb{C}$ is a complex number. Specifically, we have $E_{1,1}(z) = e^z$.

Taking the Laplace transform of (2) yields

$$\mathcal{L}\{t^{\beta-1} E_{\alpha,\beta}(-ct^\alpha)\} = \frac{s^{\alpha-\beta}}{s^\alpha + c} \tag{3}$$

For the two-parameter Mittag-Leffler function, the following two lemmas hold.

Lemma 1 [7]. For any integer $w \geq 1$, there exist real numbers $\alpha \in (0, 2)$ and $v \in (\pi\alpha/2, \min\{\pi, \pi\alpha\})$, and an arbitrary real number, β , such that

$$E_{\alpha,\beta}(z) = -\sum_{j=0}^{\infty} \frac{z^j}{\Gamma(\beta - j\alpha)z^j} + o(|z|^{-w-1}) \tag{4}$$

where $|z| \rightarrow \infty$ and $v \leq |\arg(z)| \leq \pi$, and the symbol $\arg(\cdot)$ represents the argument of a complex number.

Lemma 2 [7]. For $\alpha \in (0, 2)$, if there exist real numbers β and $v \in (\pi\alpha/2, \min\{\pi, \pi\alpha\})$, then we have

$$|E_{\alpha,\beta}(z)| \leq \frac{d}{1 + |z|} \tag{5}$$

where $d > 0$ is constant, $|z| \geq 0$ and $v \leq |\arg(z)| \leq \pi$.

Lemma 3 [10]. Let $x = 0$ be an equilibrium point of the fractional-order system ${}^c\mathcal{D}_t^\alpha x(t) = F(x(t), t)$, where $\alpha \in (0, 1)$. Assume that there exist class $-\mathcal{K}$ functions χ_1, χ_2 and χ_3 and a continuous Lyapunov function $V(x(t), t)$, such that the following inequalities

$$\chi_1(\|x(t)\|) \leq V(\|x(t), t\|) \leq \chi_2(\|x(t)\|) \tag{6}$$

and

$${}^c\mathcal{D}_t^\alpha V(x(t), t) \leq -\chi_3(\|x(t)\|) \tag{7}$$

hold; then, the origin of the system ${}^c\mathcal{D}_t^\alpha x(t) = F(x(t), t)$ is asymptotically stable.

Next, a definition and some useful lemmas for control law design are given.

Definition 3 [36]. A function $\mathcal{N}(\tau)$ is called a Nussbaum gain function if it satisfies the following properties:

$$\begin{aligned} \limsup_{s \rightarrow \infty} \frac{1}{s} \int_0^s \mathcal{N}(\tau) d\tau &= +\infty \\ \liminf_{s \rightarrow \infty} \frac{1}{s} \int_0^s \mathcal{N}(\tau) d\tau &= -\infty \end{aligned} \tag{8}$$

Lemma 4 [30]. Let $V(t)$ and $\varsigma_i(t), i = 1, \dots, m$ be smooth functions defined on $[0, t_f)$ with $V(t) \geq 0$ for $\forall t \in [0, t_f)$, and let $\xi_i(t), i = 1, \dots, m$ be unknown time-varying parameters that have the same sign and satisfy $\xi_i(t) \in \mathcal{I}_i := [\xi_{i,\min}, \xi_{i,\max}]$ with $0 \notin \mathcal{I}_i$. If the following inequality holds:

$${}^c\mathcal{D}_t^\alpha V(t) \leq -\omega V + \sum_{i=1}^m (\xi_i(t)\mathcal{N}(\varsigma_i) + 1)\dot{\varsigma}_i + \rho \tag{9}$$

then $\varsigma_i(t), V(t)$ and $\sum_{i=1}^m (\xi_i(t)\mathcal{N}(\varsigma_i) + 1)\dot{\varsigma}_i$ will be bounded on $[0, t_f)$ for $i = 1, \dots, n$, where $\omega > 0$ and $\rho > 0$ are constants. As $m = 1$, the boundedness of $(\xi(t)\mathcal{N}(\varsigma) + 1)\dot{\varsigma}$ is held.

Lemma 5 [12]. Let $x(t) \in \mathbb{R}$ be a smooth function; then, for all $t \geq t_0$, the following inequality holds:

$$\frac{1}{2} {}^c\mathcal{D}_t^\alpha (x^T(t)x(t)) \leq x^T(t) {}^c\mathcal{D}_t^\alpha x(t) \tag{10}$$

Lemma 6 (Young’s Inequality) [40]. For $\forall (x, y) \in \mathbb{R}^2$, the following inequality holds:

$$xy \leq \frac{\varepsilon^p}{p} |x|^p + \frac{1}{q\varepsilon^q} |y|^q \tag{11}$$

where $\varepsilon > 0, p > 1, q > 1$ and $(p - 1)(q - 1) = 1$.

Lemma 7 [41]. For any $\eta > 0$ and $z \in \mathbb{R}$, the following inequality holds:

$$0 \leq |z| - \frac{z^2}{\sqrt{z^2 + \eta^2}} \leq \eta \tag{12}$$

2.2. Problem Description

The subsequent discussion is based on the following type of strict-feedback fractional-order nonlinear systems:

$$\begin{aligned}
 {}^c\mathcal{D}_t^\alpha x_i(t) &= x_{i+1}(t) + \psi_i f_i(\bar{x}_i(t)) + d_i(t), \quad i = 1, \dots, n-1 \\
 {}^c\mathcal{D}_t^\alpha x_n(t) &= Q(u(t)) + \psi_n f_n(\bar{x}_n(t)) + d_n(t) \\
 y &= x_1(t)
 \end{aligned}
 \tag{13}$$

where $\bar{x}_i = [x_1, \dots, x_i]^T \in R^i, i = 1, \dots, n, u(t) \in R$ and $y \in R$ are the state vector, input and output of this system, respectively; $Q(u(t))$ is the quantized input signal of a hysteretic quantizer; $\psi_i \in R$ and $f_i(\bar{x}_i) \in R, i = 1, \dots, n$ are unknown constant parameters and known smooth functions, respectively; and $d_i(t) \in R, i = 1, \dots, n$ represents the unknown but bounded external disturbances.

With reference to [42,43], the quantized input $Q(u(t))$ can be described as the following form:

$$Q(u) = \begin{cases} \vartheta_j \text{sgn}(u), & \frac{\vartheta_j}{1+\ell} < |u| \leq \vartheta_j, \dot{u} < 0 \text{ or } \vartheta_j < |u| \leq \frac{\vartheta_j}{1-\ell}, \dot{u} > 0 \\ \vartheta_j(1+\ell)\text{sgn}(u), & \vartheta_j < |u| \leq \frac{\vartheta_j}{1-\ell}, \dot{u} < 0 \text{ or } \frac{\vartheta_j}{1-\ell} < |u| \leq \frac{\vartheta_j(1+\ell)}{1-\ell}, \dot{u} > 0 \\ 0, & 0 \leq |u| < \frac{\vartheta_{\min}}{1+\ell}, \dot{u} < 0 \text{ or } \frac{\vartheta_{\min}}{1+\ell} \leq |u| < \vartheta_{\min}, \dot{u} > 0 \\ Q(u(t^-)), & \text{otherwise} \end{cases}
 \tag{14}$$

where $\vartheta_j = \delta^{1-j}\vartheta_{\min}, j = 1, 2, \dots,$ and $\ell = (1-\delta)/(1+\delta)$ with parameters $\vartheta_{\min} > 0$ and $0 < \delta < 1$; and δ is considered to be the quantization density. Moreover, $Q(u(t))$ can be decomposed into the following form:

$$Q(u) = G(u)u(t) + P(t)
 \tag{15}$$

where $0 < 1-\delta \leq G(u) \leq 1+\delta$ and $|P(t)| \leq \vartheta_{\min}$.

The control objective of this paper was to propose an adaptive control law $u(t)$ for the strict-feedback fractional-order nonlinear systems with quantized input and external disturbances, combining the dynamic surface control method and Nussbaum gain function technique such that the output y could follow the desired signal y_d and ensure the boundedness of all signals in the given strict-feedback fractional-order nonlinear systems.

Assumption 1 [15,27,36]. *There exists an unknown positive constant \bar{d}_i , such that $|d_i(t)| \leq \bar{d}_i$ for all $t \geq 0, i = 1, \dots, n$.*

Assumption 2 [12,27,30]. *The given desired signal y_d and its fractional-order derivatives ${}^c\mathcal{D}_t^\alpha y_d$ and ${}^c\mathcal{D}_t^\alpha({}^c\mathcal{D}_t^\alpha y_d)$ are smooth, available and bounded.*

3. Adaptive Dynamic Surface Control Law Design and Stability Analysis

3.1. Adaptive Dynamic Surface Control Law Design

In this subsection, an adaptive dynamic surface control law is presented to deal with the stabilization problem of the strict-feedback fractional-order nonlinear system (13), and a stability analysis is provided as well.

For the control law design, we define the coordinate transformation as

$$\begin{aligned}
 e_1 &= x_1 - y_d \\
 e_i &= x_i - s_{i-1} \\
 z_{i-1} &= s_{i-1} - v_{i-1}
 \end{aligned}
 \tag{16}$$

where $i = 2, \dots, n; e_i$ is the surface error; s_{i-1} is the filtered output, which is yielded through a fractional-order filter on the virtual control law v_{i-1} ; and z_{i-1} represents the output error of the fractional-order filter.

In this paper, the fractional-order filter design was inspired by the work of [43]. Let the virtual control law $v_i, i = 1, \dots, n - 1$ pass through the following fractional-order filter with a time constant τ_i to yield the filtered output s_i , that is

$$\tau_i {}^c \mathcal{D}_t^\alpha s_i = -z_i - \frac{\tau_i \hat{\Pi}_i^2 z_i}{\sqrt{(\hat{\Pi}_i z_i)^2 + \eta^2(t)}} - \tau_i e_i \tag{17}$$

where $i = 1, \dots, n - 1$ and $\hat{\Pi}_i$ is the estimation of Π_i , which will be defined later.

Step 1 ($i = 1$). In view of (13) and (16), the a th-order derivative of e_1 is obtained as

$${}^c \mathcal{D}_t^\alpha e_1 = e_2 + v_1 + z_1 + \psi_1 f_1 + d_1(t) - {}^c \mathcal{D}_t^\alpha y_d \tag{18}$$

The design of the following Lyapunov function candidate is

$$V_1 = \frac{1}{2} e_1^2 + \frac{1}{2\beta_1} \tilde{\psi}_1^2 + \frac{1}{2\gamma_1} \tilde{\Delta}_1^2 \tag{19}$$

where $\beta_1 > 0$ and $\gamma_1 > 0$ are design parameters, $\tilde{\psi}_1 = \hat{\psi}_1 - \psi_1, \tilde{\Delta}_1 = \hat{\Delta}_1 - \Delta_1$ and $\hat{\psi}_1$ and $\hat{\Delta}_1$ are the estimations of ψ_1 and $\Delta_1 = \bar{d}_1$, respectively.

Along with (18) and Lemma 5, the a th-order derivative of V_1 is given as

$${}^c \mathcal{D}_t^\alpha V_1 \leq e_1 (e_2 + v_1 + z_1 + \psi_1 f_1 + d_1(t) - {}^c \mathcal{D}_t^\alpha y_d) + \frac{1}{\beta_1} \tilde{\psi}_1 {}^c \mathcal{D}_t^\alpha \hat{\psi}_1 + \frac{1}{\gamma_1} \tilde{\Delta}_1 {}^c \mathcal{D}_t^\alpha \hat{\Delta}_1 \tag{20}$$

The design of the virtual control law v_1 is

$$v_1 = -a_1 e_1 - \hat{\psi}_1 f_1 - \frac{\hat{\Delta}_1 e_1}{\sqrt{e_1^2 + \eta^2(t)}} + {}^c \mathcal{D}_t^\alpha y_d \tag{21}$$

where $a_1 > 0$ is a design parameter and $\eta = \eta(t)$ represents a positive uniform continuous and bounded function.

With reference to [28], there exist constants $\lambda_1 > 0$ and $\lambda_2 > 0$, such that

$$0 < \eta(t) < \lambda_1 < +\infty, |{}^c \mathcal{D}_t^\alpha \eta(t)| < \lambda_2 < +\infty \tag{22}$$

Let v_1 pass through the fractional-order filter (17) to obtain the filtered output s_1 , then one has

$$\tau_1 {}^c \mathcal{D}_t^\alpha s_1 = -z_1 - \frac{\tau_1 \hat{\Pi}_1^2 z_1}{\sqrt{(\hat{\Pi}_1 z_1)^2 + \eta^2(t)}} - \tau_1 e_1, s_1(0) = v_1(0) \tag{23}$$

Substituting (21) into (20), we obtain

$${}^c \mathcal{D}_t^\alpha V_1 \leq -a_1 e_1^2 + \frac{1}{\beta_1} \tilde{\psi}_1 ({}^c \mathcal{D}_t^\alpha \hat{\psi}_1 - \beta_1 e_1 f_1) + \frac{1}{\gamma_1} \tilde{\Delta}_1 \left({}^c \mathcal{D}_t^\alpha \hat{\Delta}_1 - \frac{\gamma_1 e_1^2}{\sqrt{e_1^2 + \eta^2(t)}} \right) + e_1 (e_2 + z_1) + \Delta_1 \lambda_1 \tag{24}$$

where $e_1 d_1(t) \leq |e_1| \Delta_1 \leq \Delta_1 \eta(t) + \Delta_1 e_1^2 / \sqrt{e_1^2 + \eta^2(t)}$ is considered using Lemma 7.

The adaptive laws ${}^c \mathcal{D}_t^\alpha \hat{\psi}_1$ and ${}^c \mathcal{D}_t^\alpha \hat{\Delta}_1$ are

$${}^c \mathcal{D}_t^\alpha \hat{\psi}_1 = \beta_1 e_1 f_1 - c_1 \hat{\psi}_1 \tag{25}$$

$${}^c \mathcal{D}_t^\alpha \hat{\Delta}_1 = \frac{\gamma_1 e_1^2}{\sqrt{e_1^2 + \eta^2(t)}} - g_1 \hat{\Delta}_1 \tag{26}$$

Substituting (25) and (26) into (24), we have

$${}^c\mathcal{D}_t^\alpha V_1 \leq -a_1 e_1^2 - \frac{c_1}{\beta_1} \tilde{\psi}_1 \hat{\psi}_1 - \frac{g_1}{\gamma_1} \tilde{\Delta}_1 \hat{\Delta}_1 + e_1(e_2 + z_1) + \Delta_1 \lambda_1 \tag{27}$$

Step i ($i = 2, \dots, n - 1$). From (16), the i th-order derivative of e_i is as follows:

$${}^c\mathcal{D}_t^\alpha e_i = e_{i+1} + v_i + z_i + \psi_i f_i + d_i(t) - {}^c\mathcal{D}_t^\alpha s_{i-1} \tag{28}$$

The design of the following Lyapunov function candidate is

$$V_i = \frac{1}{2} e_i^2 + \frac{1}{2\beta_i} \tilde{\psi}_i^2 + \frac{1}{2\gamma_i} \tilde{\Delta}_i^2 \tag{29}$$

where $\beta_i > 0$ and $\gamma_i > 0$ are design parameters, $\tilde{\psi}_i = \hat{\psi}_i - \psi_i$, $\tilde{\Delta}_i = \hat{\Delta}_i - \Delta_i$ and $\hat{\psi}_i$ and $\hat{\Delta}_i$ are the estimations of ψ_i and $\Delta_i = \bar{d}_i$, respectively.

Similar to Step 1, and along with (28), the i th-order derivative of V_i is

$${}^c\mathcal{D}_t^\alpha V_i \leq e_i(e_{i+1} + v_i + z_i + \psi_i f_i + d_i(t) - {}^c\mathcal{D}_t^\alpha s_{i-1}) + \frac{1}{\beta_i} \tilde{\psi}_i {}^c\mathcal{D}_t^\alpha \hat{\psi}_i + \frac{1}{\gamma_i} \tilde{\Delta}_i {}^c\mathcal{D}_t^\alpha \hat{\Delta}_i \tag{30}$$

The design of the virtual control law v_i is

$$v_i = -a_i e_i - \hat{\psi}_i f_i - \frac{\hat{\Delta}_i e_i}{\sqrt{e_i^2 + \eta^2(t)}} - \frac{z_{i-1}}{\tau_{i-1}} - \frac{\hat{\Pi}_{i-1}^2 z_{i-1}}{\sqrt{(\hat{\Pi}_{i-1} z_{i-1})^2 + \eta^2(t)}} - 2e_{i-1} \tag{31}$$

where $a_i > 0$ is a design parameter and $\hat{\Pi}_{i-1}$ represents the estimation of Π_{i-1} , which will be defined later.

Letting v_i pass through the fractional-order filter (17) to obtain the filtered output s_i , one has

$$\tau_i {}^c\mathcal{D}_t^\alpha s_i = -z_i - \frac{\tau_i \hat{\Pi}_i^2 z_i}{\sqrt{(\hat{\Pi}_i z_i)^2 + \eta^2(t)}} - \tau_i e_i, \quad s_i(0) = v_i(0) \tag{32}$$

The adaptive laws ${}^c\mathcal{D}_t^\alpha \hat{\psi}_i$ and ${}^c\mathcal{D}_t^\alpha \hat{\Delta}_i$ are

$${}^c\mathcal{D}_t^\alpha \hat{\psi}_i = \beta_i e_i f_i - c_i \hat{\psi}_i \tag{33}$$

$${}^c\mathcal{D}_t^\alpha \hat{\Delta}_i = \frac{\gamma_i e_i^2}{\sqrt{e_i^2 + \eta^2(t)}} - g_i \hat{\Delta}_i \tag{34}$$

In addition, using Lemma 7, we have

$$e_i d_i(t) \leq |e_i| \Delta_i \leq \Delta_i \eta(t) + \frac{\Delta_i e_i^2}{\sqrt{e_i^2 + \eta^2(t)}} \tag{35}$$

Substituting (31)–(35) into (30), the following can be obtained:

$${}^c\mathcal{D}_t^\alpha V_i \leq -a_i e_i^2 - \frac{c_i}{\beta_i} \tilde{\psi}_i \hat{\psi}_i - \frac{g_i}{\gamma_i} \tilde{\Delta}_i \hat{\Delta}_i + e_i(e_{i+1} + z_i - e_{i-1}) + \Delta_i \lambda_1 \tag{36}$$

Step n ($i = n$). This is the last step, in which the actual control law $u(t)$ will be developed using the dynamic surface control technique and Nussbaum gain function technique. Invoking (14)–(16), the n th-order derivative of e_n is

$${}^c\mathcal{D}_t^\alpha e_n = G(u)u(t) + \psi_n f_n + P(t) + d_n(t) - {}^c\mathcal{D}_t^\alpha s_{n-1} \tag{37}$$

The design of the following Lyapunov function candidate is

$$V_n = \frac{1}{2}e_n^2 + \frac{1}{2\beta_n}\tilde{\psi}_n^2 + \frac{1}{2\gamma_n}\tilde{\Delta}_n^2 \tag{38}$$

where $\beta_n > 0$ and $\gamma_n > 0$ are design parameters, $\tilde{\psi}_n = \hat{\psi}_n - \psi_n$, $\tilde{\Delta}_n = \hat{\Delta}_n - \Delta_n$ and $\hat{\psi}_n$ and $\hat{\Delta}_n$ are the estimations of ψ_n and $\Delta_n = \vartheta_{\min} + \bar{d}_n$, respectively.

Taking the a th-order derivative of V_n along with (37) yields

$${}^c\mathcal{D}_t^\alpha V_n \leq \sigma e_n \bar{G}(u)u(t) + e_n(\psi_n f_n + P(t) + d_n(t) - {}^c\mathcal{D}_t^\alpha s_{n-1}) + \frac{1}{\beta_n}\tilde{\psi}_n {}^c\mathcal{D}_t^\alpha \hat{\psi}_n + \frac{1}{\gamma_n}\tilde{\Delta}_n {}^c\mathcal{D}_t^\alpha \hat{\Delta}_n \tag{39}$$

where $\bar{G}(u) = G(u)/\sigma$ and $\sigma > 0$ is the introduced adjustment coefficient, which is used to adjust the control law.

Remark 1. As $0 < 1 - \delta \leq G(u) \leq 1 + \delta$, the explicit value of $G(u)$ is not easy to obtain. Therefore, the Nussbaum gain function technique is introduced to deal with the unknown control gain and design the control law $u(t)$.

Let v_{n-1} pass through the fractional-order filter (17) to obtain the filtered output s_{n-1} , then one has

$$\tau_{n-1} {}^c\mathcal{D}_t^\alpha s_{n-1} = -z_{n-1} - \frac{\tau_{n-1}\hat{\Pi}_{n-1}^2 z_{n-1}}{\sqrt{(\hat{\Pi}_{n-1} z_{n-1})^2 + \eta^2(t)}} - \tau_{n-1}e_{n-1}, s_{n-1}(0) = v_{n-1}(0) \tag{40}$$

where $\hat{\Pi}_{n-1}$ represents the estimation of Π_{n-1} , which will be defined later.

The design of the actual control law $u(t)$ is

$$u(t) = \mathcal{N}(\varsigma)\varphi(t) \tag{41}$$

where $\mathcal{N}(\varsigma)$ is a given Nussbaum gain function, and $\varphi(t)$ and adaptive law $\dot{\varsigma}(t)$ are given, respectively, as

$$\varphi(t) = \frac{1}{\sigma} \left(a_n e_n + \hat{\psi}_n f_n + \frac{\hat{\Delta}_n e_n}{\sqrt{e_n^2 + \eta^2(t)}} + \frac{z_{n-1}}{\tau_{n-1}} + \frac{\hat{\Pi}_{n-1}^2 z_{n-1}}{\sqrt{(\hat{\Pi}_{n-1} z_{n-1})^2 + \eta^2(t)}} + 2e_{n-1} \right) \tag{42}$$

$$\dot{\varsigma}(t) = \sigma e_n \varphi(t) \tag{43}$$

where $a_n > 0$ is a design parameter.

The adaptive laws ${}^c\mathcal{D}_t^\alpha \hat{\psi}_n$ and ${}^c\mathcal{D}_t^\alpha \hat{\Delta}_n$ are

$${}^c\mathcal{D}_t^\alpha \hat{\psi}_n = \beta_n e_n f_n - c_n \hat{\psi}_n \tag{44}$$

$${}^c\mathcal{D}_t^\alpha \hat{\Delta}_n = \frac{\gamma_n e_n^2}{\sqrt{e_n^2 + \eta^2(t)}} - g_n \hat{\Delta}_n \tag{45}$$

Using Lemma 7, one has

$$e_n(P(t) + d_n(t)) \leq |e_n|(\vartheta_{\min} + \bar{d}_n) = |e_n|\Delta_n \leq \Delta_n \eta(t) + \frac{\Delta_n e_n^2}{\sqrt{e_n^2 + \eta^2(t)}} \tag{46}$$

Substituting (40)–(46) into (39), we obtain

$${}^c\mathcal{D}_t^\alpha V_n \leq -a_n e_n^2 - \frac{c_n}{\beta_n}\tilde{\psi}_n \hat{\psi}_n - \frac{g_n}{\gamma_n}\tilde{\Delta}_n \hat{\Delta}_n - e_{n-1}e_n + \Delta_n \lambda_1 + (\bar{G}(u)\mathcal{N}(\varsigma) + 1)\dot{\varsigma}(t) \tag{47}$$

Remark 2. The nonlinear terms $\hat{\Delta}_i e_i / \sqrt{e_i^2 + \eta^2(t)}$ and $i = 1, \dots, n$ in the virtual control law and actual control law are used to compensate for the bound of external disturbances $d_i(t)$, $i = 1, \dots, n$ and the unknown bounded function $P(t)$, where the introduction of the adjusting function $\eta(t)$ is used to overcome a possible chattering problem in the virtual control laws and the actual control law. According to [28], $\eta(t)$ can be considered an exponential function, for example, $\eta(t) = \lambda_1 e^{-\lambda_2 t}$ (λ_1 and λ_2 are positive constants), which satisfies $0 < \eta(t) < \lambda_1 < +\infty$ and $|{}^c \mathcal{D}_t^\alpha \eta(t)| < \lambda_2 < +\infty$.

Remark 3. The nonlinear function $\hat{\Pi}_i^2 z_i / \sqrt{(\hat{\Pi}_i z_i)^2 + \eta^2(t)}$, $i = 1, \dots, n-1$ with an adaptive law for $\hat{\Pi}_i$ is designed in each fractional-order nonlinear filter and is used to compensate for the effect caused by surface error. Furthermore, the nonlinear function is introduced into the fractional-order nonlinear filter, which can also avoid the complexity explosion problem caused by repeatedly differentiating the virtual control law v_i .

3.2. Stability Analysis

Based on the above analysis, the main results of this work can be summarized as follows.

Theorem 1. Consider the strict-feedback fractional-order nonlinear systems (13) with input quantization and external disturbances. Under Assumptions 1 and 2, the virtual control laws are constructed as in (21) and (31); the adaptive laws are considered as in (25), (26), (33), (34), (44) and (45); and the actual control law is designed as in (41) with (42) and (43). Then, the following results are obtained: (i) the boundedness of all signals of the strict-feedback fractional-order systems (13) are obtained and (ii) the tracking error can converge to an arbitrary small neighborhood of the origin.

Proof. From (16) and (17), the a th-order derivative of z_i is

$$\begin{aligned} {}^c \mathcal{D}_t^\alpha z_i &= {}^c \mathcal{D}_t^\alpha s_i - {}^c \mathcal{D}_t^\alpha v_i \\ &= -\frac{z_i}{\tau_i} - \frac{\hat{\Pi}_i^2 z_i}{\sqrt{(\hat{\Pi}_i z_i)^2 + \eta^2(t)}} - e_i + H_i(\cdot), \quad i = 1, \dots, n-1 \end{aligned} \quad (48)$$

where $H_i(\cdot)$ is a continuous function with variables $e_1, \dots, e_{i+1}, z_1, \dots, z_i, \hat{\psi}_1, \dots, \hat{\psi}_{i+1}, \hat{\Delta}_1, \dots, \hat{\Delta}_{i+1}, \hat{\Pi}_1, \dots, \hat{\Pi}_i, y_d, {}^c \mathcal{D}_t^\alpha y_d, {}^c \mathcal{D}_t^\alpha ({}^c \mathcal{D}_t^\alpha y_d), \eta(t)$ and $\dot{\eta}(t)$.

The following Lyapunov function candidate is constructed:

$$V = \sum_{i=1}^n V_i + \sum_{i=1}^{n-1} \frac{1}{2} z_i^2 + \sum_{i=1}^{n-1} \frac{1}{2\lambda_i} \tilde{\Pi}_i^2 \quad (49)$$

where $\lambda_i > 0$ and $i = 1, \dots, n-1$ are design parameters, and $\tilde{\Pi}_i = \hat{\Pi}_i - \Pi_i$ and $\hat{\Pi}_i$ are estimations of Π_i .

In addition, considering Assumption 2, there exists a compact set

$$\Omega_1 = \left\{ (y_d)^2 + ({}^c \mathcal{D}_t^\alpha y_d)^2 + ({}^c \mathcal{D}_t^\alpha ({}^c \mathcal{D}_t^\alpha y_d))^2 \leq Y_0 \right\} \quad (50)$$

where $Y_0 > 0$ is a known constant.

Furthermore, we define the following compact set as

$$\Omega_2 = \{V(t) \leq q\} \quad (51)$$

where $q > 0$ represents any constant.

Noting (50) and (51), it can be found that the set $\Omega_1 \times \Omega_2$ is also a compact set, and that $\eta(t)$ and $\dot{\eta}(t)$ are bounded functions. Therefore, there exist positive constants Π_i ,

$i = 1, \dots, n - 1$, such that $|H_i(\cdot)| \leq \Pi_i$ on $\Omega_1 \times \Omega_2$, since the determined values of Π_i are not easy to obtain, which are estimated by $\hat{\Pi}_i$.

The n th-order derivative of V is

$${}^c \mathcal{D}_t^\alpha V \leq \sum_{i=1}^n {}^c \mathcal{D}_t^\alpha V_i + \sum_{i=1}^{n-1} z_i {}^c \mathcal{D}_t^\alpha z_i + \sum_{i=1}^{n-1} \frac{1}{\lambda_i} \tilde{\Pi}_i {}^c \mathcal{D}_t^\alpha \hat{\Pi}_i \tag{52}$$

Substituting (27), (36), (47) and (48) into (52), we have

$$\begin{aligned} {}^c \mathcal{D}_t^\alpha V \leq & - \sum_{i=1}^n a_i e_i^2 - \sum_{i=1}^n \frac{c_i}{\beta_i} \tilde{\psi}_i \hat{\psi}_n - \sum_{i=1}^n \frac{g_i}{\gamma_i} \tilde{\Delta}_i \hat{\Delta}_i - \sum_{i=1}^{n-1} \frac{z_i^2}{\tau_i} + \lambda_1 \sum_{i=1}^n \Delta_i + (\bar{G}(u)\mathcal{N}(\zeta) + 1)\dot{\zeta}(t) \\ & + \sum_{i=1}^{n-1} |z_i| \Pi_i - \sum_{i=1}^{n-1} \frac{\hat{\Pi}_i^2 z_i^2}{\sqrt{(\hat{\Pi}_i z_i)^2 + \eta^2(t)}} + \sum_{i=1}^{n-1} \frac{1}{\lambda_i} \tilde{\Pi}_i {}^c \mathcal{D}_t^\alpha \hat{\Pi}_i \end{aligned} \tag{53}$$

Using Lemma 7, the following can be obtained

$$|z_i| \Pi_i = |z_i| \hat{\Pi}_i - |z_i| \tilde{\Pi}_i \leq \frac{\hat{\Pi}_i^2 z_i^2}{\sqrt{(\hat{\Pi}_i z_i)^2 + \eta^2(t)}} + \eta(t) - |z_i| \tilde{\Pi}_i \tag{54}$$

Then, one has

$$\begin{aligned} {}^c \mathcal{D}_t^\alpha V \leq & - \sum_{i=1}^n a_i e_i^2 - \sum_{i=1}^n \frac{c_i}{\beta_i} \tilde{\psi}_i \hat{\psi}_n - \sum_{i=1}^n \frac{g_i}{\gamma_i} \tilde{\Delta}_i \hat{\Delta}_i - \sum_{i=1}^{n-1} \frac{z_i^2}{\tau_i} + \sum_{i=1}^{n-1} \frac{1}{\lambda_i} \tilde{\Pi}_i ({}^c \mathcal{D}_t^\alpha \hat{\Pi}_i - \lambda_i |z_i|) \\ & + \lambda_1 \sum_{i=1}^n \Delta_i + \lambda_1 (n - 1) + (\bar{G}(u)\mathcal{N}(\zeta) + 1)\dot{\zeta}(t) \end{aligned} \tag{55}$$

The adaptive law ${}^c \mathcal{D}_t^\alpha \hat{\Pi}_i$ is

$${}^c \mathcal{D}_t^\alpha \hat{\Pi}_i = \lambda_i |z_i| - k_i \hat{\Pi}_i, \quad i = 1, \dots, n - 1 \tag{56}$$

where $k_i > 0$ is a design parameter.

In addition, by applying Lemma 6, the following inequalities are obtained:

$$- \frac{c_i}{\beta_i} \tilde{\psi}_i \hat{\psi}_n \leq - \frac{c_i}{2\beta_i} \tilde{\psi}_i^2 + \frac{c_i}{2\beta_i} \psi_i^2 \tag{57}$$

$$- \frac{g_i}{\gamma_i} \tilde{\Delta}_i \hat{\Delta}_i \leq - \frac{g_i}{2\gamma_i} \tilde{\Delta}_i^2 + \frac{g_i}{2\gamma_i} \Delta_i^2 \tag{58}$$

$$- \frac{k_i}{\lambda_i} \tilde{\Pi}_i \hat{\Pi}_i \leq - \frac{k_i}{2\lambda_i} \tilde{\Pi}_i^2 + \frac{k_i}{2\lambda_i} \Pi_i^2 \tag{59}$$

Substituting (56)–(59) into (55), we have

$${}^c \mathcal{D}_t^\alpha V \leq -\phi V + (\bar{G}(u)\mathcal{N}(\zeta) + 1)\dot{\zeta}(t) + D_1 \tag{60}$$

where $\phi = \min\{2a_i, c_i, g_i, 2/\tau_j, k_j\}$, for $i = 1, \dots, n$ and $j = 1, \dots, n - 1$, and

$$D_1 = \sum_{i=1}^n \frac{c_i}{2\beta_i} \psi_i^2 + \sum_{i=1}^n \frac{g_i}{2\gamma_i} \Delta_i^2 + \sum_{i=1}^{n-1} \frac{k_i}{2\lambda_i} \Pi_i^2 + \lambda_1 \sum_{i=1}^n \Delta_i + \lambda_1 (n - 1) \tag{61}$$

Furthermore, considering Lemma 4 and letting $m = 1$, it can be easily seen that there exists a positive constant, D_2 , such that $\max(\bar{G}(u)\mathcal{N}(\zeta) + 1) = D_2$. Let $D = D_1 + D_2$, then we have

$${}^c \mathcal{D}_t^\alpha V \leq -\phi V + D \tag{62}$$

From (62), there must exist a positive time-varying parameter, $\zeta(t)$, such that

$${}^c \mathcal{D}_t^\alpha V(t) + \zeta(t) = -\phi V(t) + D \tag{63}$$

Taking the Laplace transform of (63) yields

$$V(s) = \frac{s^{\alpha-1}}{s^\alpha + \phi} V(0) + \frac{D}{s(s^\alpha + \phi)} - \frac{\Xi(s)}{s^\alpha + \phi} = \frac{s^{\alpha-1}}{s^\alpha + \phi} V(0) + \frac{s^{\alpha-(\alpha-1)}}{s^\alpha + \phi} D - \frac{\Xi(s)}{s^\alpha + \phi} \tag{64}$$

where $V(s)$ and $\Xi(s)$ are the Laplace transforms of $V(t)$ and $\Xi(s)$, respectively.

Considering Definition 2, the inverse Laplace transform of (64) is

$$V(t) = E_{a,1}(-\phi t^\alpha) V(0) + t^\alpha E_{a,\alpha+1}(-\phi t^\alpha) D - \zeta(t) * t^{\alpha-1} E_{a,\alpha}(-\phi t^\alpha) \tag{65}$$

where the symbol $*$ stands for the convolution operator.

As $\zeta(t)$ is a non-negative parameter, and from the definition of the two-parameter Mittag-Leffler function (2), it can be directly obtained that $t^{\alpha-1} E_{a,\alpha}(-\phi t^\alpha) > 0$. As a result, from (65), we have $-\zeta(t) * t^{\alpha-1} E_{a,\alpha}(-\phi t^\alpha) \leq 0$. Thus, the equation (65) is changed is

$$V(t) \leq E_{a,1}(-\phi t^\alpha) V(0) + t^\alpha E_{a,\alpha+1}(-\phi t^\alpha) D \tag{66}$$

On the other hand, for all $t \geq 0$, one has $\arg(-\phi t^\alpha) = -\pi$ and $|\phi t^\alpha| \geq 0$. Then, from Lemma 2, there must exist a constant, $d > 0$, such that the following inequality holds:

$$|E_{a,1}(-\phi t^\alpha)| \leq \frac{d}{1 + \phi t^\alpha} \tag{67}$$

With $t \rightarrow \infty$, we have

$$\lim_{t \rightarrow \infty} E_{a,1}(-\phi t^\alpha) V(0) = 0 \tag{68}$$

Observing (68), for any $\bar{h} > 0$, there exists a time instant $t_1 > 0$ for all $t > t_1$, such that

$$E_{a,1}(-\phi t^\alpha) V(0) \leq \frac{\bar{h}}{3} \tag{69}$$

Furthermore, considering Lemma 1 and letting $w = 1$, one has

$$E_{a,\alpha+1}(-\phi t^\alpha) = \frac{1}{\Gamma(1)\phi t^\alpha} + o\left(\frac{1}{|\phi t^\alpha|^2}\right) \tag{70}$$

In view of the fact that $\Gamma(1) = 1$, then (70) can be rewritten as

$$t^\alpha E_{a,\alpha+1}(-\phi t^\alpha) D = \frac{D}{\phi} + Dt^\alpha o\left(\frac{1}{|\phi t^\alpha|^2}\right) \tag{71}$$

Similarly, from (71), for any $\bar{h} > 0$, there exists a time instant $t_2 > 0$ for all $t > t_2$, such that the following inequality satisfies

$$Dt^\alpha o\left(\frac{1}{|\phi t^\alpha|^2}\right) \leq \frac{\bar{h}}{3} \tag{72}$$

In addition, we can select appropriate design parameters such that $D/\phi \leq \bar{h}/3$. Thus, invoking (66), (69) and (72), one obtains

$$V(t) \leq \bar{h} \tag{73}$$

Therefore, according to Lemma 3 and the definition of $V(t)$, once (62) and (72) hold, the boundedness of all signals of the considered strict-feedback fractional-order systems (13) is obtained, and the tracking error can also converge to an arbitrary small neighborhood of the origin, namely, $|e_1| \leq \sqrt{2\bar{h}}$ for all $t > \max\{t_1, t_2\}$. This completes the proof. \square

The control block diagram of the system is given in Figure 1.

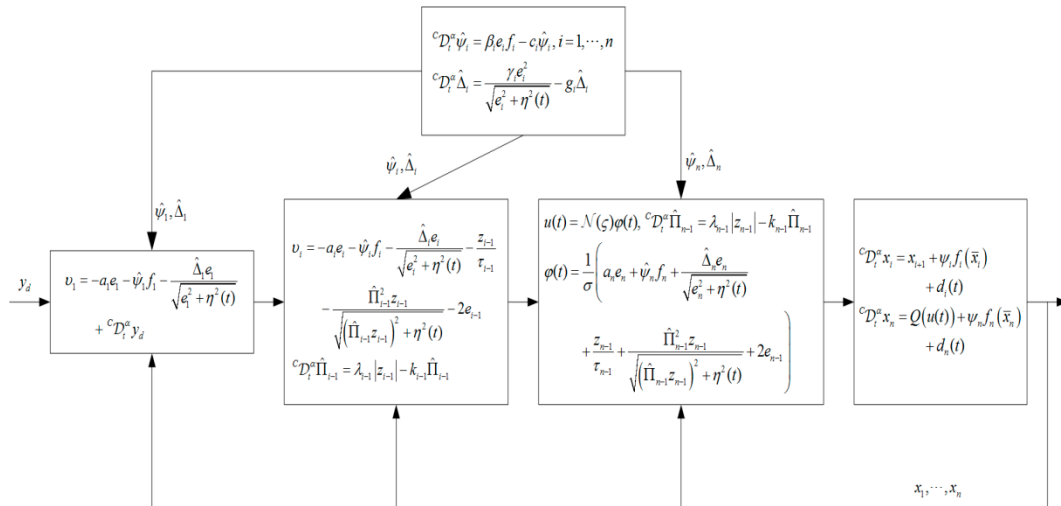


Figure 1. Block diagram of control system.

Remark 4. The theoretical analysis shows that the tracking error $|e_1| \leq \sqrt{2\bar{h}}$. Actually, it can be made arbitrarily small by increasing the design parameters a_i , β_i , γ_i and λ_i , or by decreasing the value of $\eta(t)$ under the fixed positive parameters c_i , g_i and k_i . In addition, the control law $u(t)$ can also be adjusted by changing the value of parameter σ . However, if the correction parameters are too small, the parameters may drift to some extent, and a smaller tracking error will cause a larger control amplitude. Therefore, the design parameters should be appropriately selected to trade-off between the tracking performance and magnitude of the control signal.

4. Simulation Environment and Methods

In this section, two simulation examples are provided, which were established in the environment of MATLAB/SIMULINK (MathWorks.Inc., Natick, MA, USA) to illustrate the effectiveness of the presented adaptive dynamic surface control law.

Example 1. Consider the strict-feedback fractional-order nonlinear systems with the following form:

$$\begin{aligned} {}^c\mathcal{D}_t^\alpha x_1 &= x_2 - 0.5x_1^2 + d_1(t) \\ {}^c\mathcal{D}_t^\alpha x_2 &= Q(u) + 2e^{-x_1}x_2 + d_2(t) \end{aligned} \tag{74}$$

where the fractional order α is set to 0.95 and the external disturbances are $d_1(t) = d_2(t) = 0.1 \sin(t)$. The values of the hysteretic quantizer as designed are $\vartheta_{\min} = 0.02$, $\delta = 0.5$ and $\ell = 1/3$. The initial states are considered to be $x(0) = [0.5, 0.1]^T$ and the other initial conditions are all given as 0.01. The desired signal is $y_d = 0.5 \sin(1.5t)$ and the simulation time is $t = 15$ s.

We design the first virtual control law as follows:

$$v_1 = -70e_1 - \hat{\psi}_1(x_1^2) - \frac{\hat{\Delta}_1 e_1}{\sqrt{e_1^2 + 2.5^2}} + {}^c\mathcal{D}_t^\alpha y_d \tag{75}$$

To overcome the explosion of complexity in the recursive design, a fractional-order filter is designed as

$${}^c\mathcal{D}_t^\alpha s_1 = -100z_1 - \frac{\hat{\Gamma}_1^2 z_1}{\sqrt{(\hat{\Gamma}_1 z_1)^2 + 2.5^2}} - e_1 \quad (76)$$

Furthermore, we design the actual control law and adaptive laws as

$$u(t) = \mathcal{N}(\varsigma)\varphi(t) \quad (77)$$

$$\varphi(t) = 2 \left(5e_2 + \hat{\psi}_2(e^{-x_1}x_2) + \frac{\hat{\Delta}_2 e_2}{\sqrt{e_2^2 + 2.5^2}} + 100z_1 + \frac{\hat{\Gamma}_1^2 z_1}{\sqrt{(\hat{\Gamma}_1 z_1)^2 + 2.5^2}} + 2e_1 \right) \quad (78)$$

$$\dot{\varsigma}(t) = 0.5e_2\varphi(t) \quad (79)$$

$${}^c\mathcal{D}_t^\alpha \hat{\psi}_1 = e_1(x_1^2) - 3\hat{\psi}_1 \quad (80)$$

$${}^c\mathcal{D}_t^\alpha \hat{\psi}_2 = e_2(e^{-x_1}x_2) - 2\hat{\psi}_2 \quad (81)$$

$${}^c\mathcal{D}_t^\alpha \hat{\Delta}_1 = \frac{5.5e_1^2}{\sqrt{e_1^2 + 2.5^2}} - 1.3\hat{\Delta}_1 \quad (82)$$

$${}^c\mathcal{D}_t^\alpha \hat{\Delta}_2 = \frac{1.5e_2^2}{\sqrt{e_2^2 + 2.5^2}} - 4\hat{\Delta}_2 \quad (83)$$

$${}^c\mathcal{D}_t^\alpha \hat{\Gamma}_1 = 2.5|z_1| - \hat{\Gamma}_1 \quad (84)$$

where the Nussbaum gain function is given as $\mathcal{N}(\varsigma) = \varsigma^2 \cos(\varsigma)$.

To further illustrate the validity of the presented control law, a third-order fractional-order nonlinear system is given in Example 2.

Example 2. Consider the fractional-order systems with the following form:

$$\begin{aligned} {}^c\mathcal{D}_t^\alpha x_1 &= x_2 - 2e^{-x_1/20} + d_1(t) \\ {}^c\mathcal{D}_t^\alpha x_2 &= x_3 - 0.5x_2 \sin(x_1) + d_2(t) \\ {}^c\mathcal{D}_t^\alpha x_3 &= Q(u(t)) + 0.5 \cos(x_1 x_3) + d_3(t) \end{aligned} \quad (85)$$

Let the external disturbances $d_1(t) = d_2(t) = d_3(t) = 0.1 \sin(t)$. The values of the hysteretic quantizer as designed are $\vartheta_{\min} = 0.02$, $\delta = 0.25$ and $\ell = 1/3$. The initial states are considered to be $x(0) = [0.5, 0.25, 0.1]^T$ and the others are all set to 0.01. The desired signal is $y_d = 1.5(\sin(t) + \sin(2t))$ and the simulation time is $t = 15$ s.

In order to achieve the control goal, the design parameters in the virtual control laws (see (21) and (32)), adaptive laws (see (25), (26), (33), (34), (44), (45) and (56)), actual control law (see (41)–(43)) and fractional-order filter (see (23) and (32)) were set to $a_1 = 90$, $a_2 = 35$, $a_3 = 11.5$, $\beta_1 = 30$, $\beta_2 = 23$, $\beta_3 = 20$, $c_1 = 2$, $c_2 = 5$, $c_3 = 12$, $\gamma_1 = 22$, $\gamma_2 = 13$, $\gamma_3 = 13$, $g_1 = 22.5$, $g_2 = 12$, $g_3 = 24$, $\tau_1 = \tau_2 = 0.02$, $\lambda_1 = 0.1$, $\lambda_2 = 2$, $k_1 = k_2 = 0.2$, $\sigma = 0.2$ and $\eta(t) = 2.5$.

5. Results and Discussion

Based on the examples in Section 4, the simulation results and discussion are provided in this section.

Considering Example 1, the simulation results are shown in Figures 2–7.

Figures 2 and 3 give the trajectories of the tracking performance and tracking error, respectively, and demonstrate that the system (74) could be stabilized quickly under the presented control law. In addition, it can be seen from Figures 2 and 3 that the tracking

error could converge on the small neighborhood of the origin. In other words, although the system was affected by external disturbances and input quantization, the designed control law for system (74) in this paper could still achieve good control performance, which showed the effectiveness of the proposed control law. Figure 4 shows the trajectories of the control law and quantized control input, which firmly verified the fact mentioned in Remark 4, that is, a compromise was achieved between a high control gain and tracking error. In addition, the trajectories of adaptive laws $\hat{\psi}_i$, $\hat{\Delta}_i$ and $\hat{\Pi}_1$ are shown in Figures 5–7, respectively.

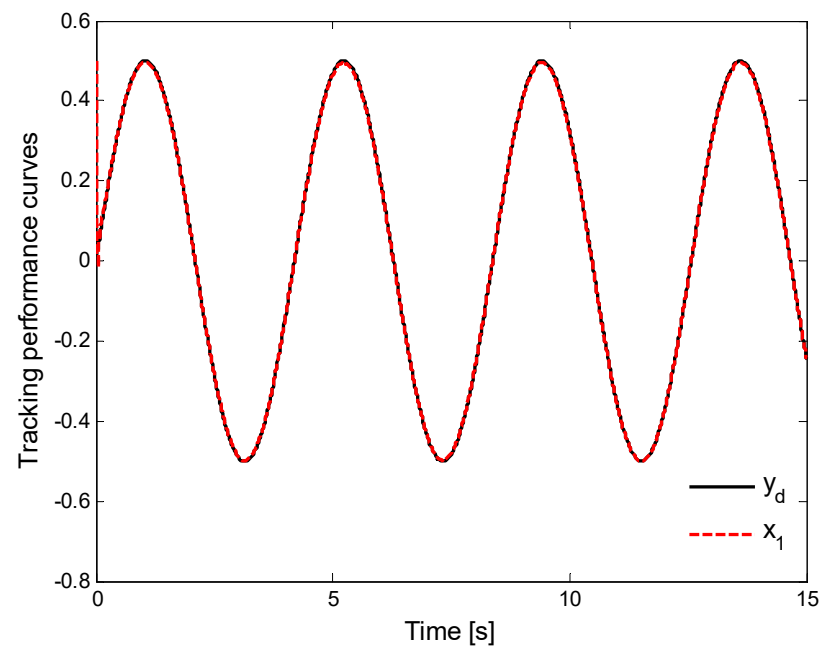


Figure 2. Trajectories of system output $x_1(t)$ and desired signal y_d .

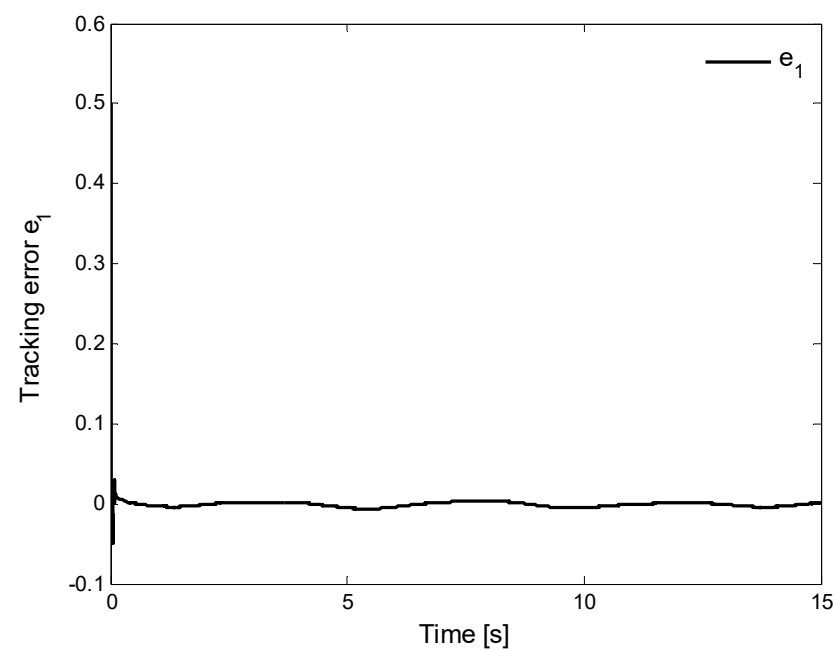


Figure 3. Trajectory of tracking error $e_1(t)$.

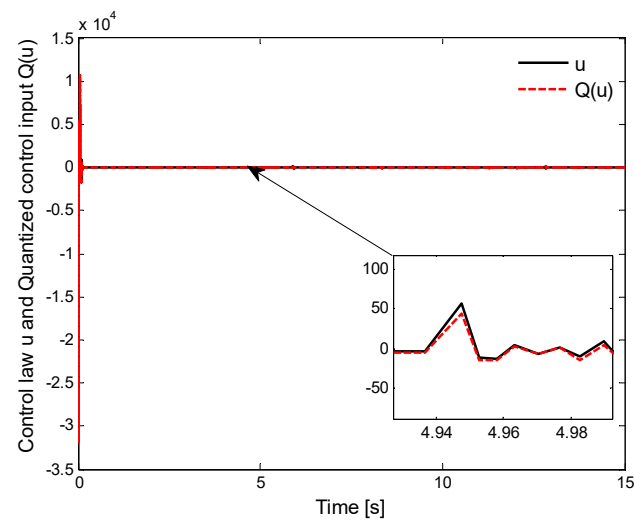


Figure 4. Trajectories of control law $u(t)$ and quantized control input $Q(u)$.

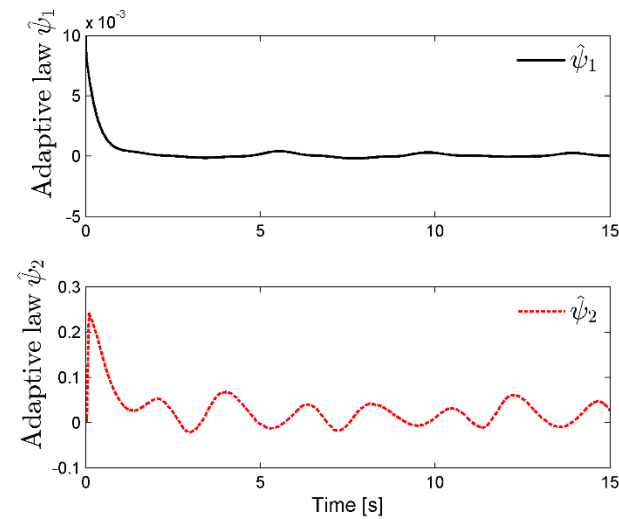


Figure 5. Trajectories of adaptive law $\hat{\psi}_i$ ($i = 1, 2$).

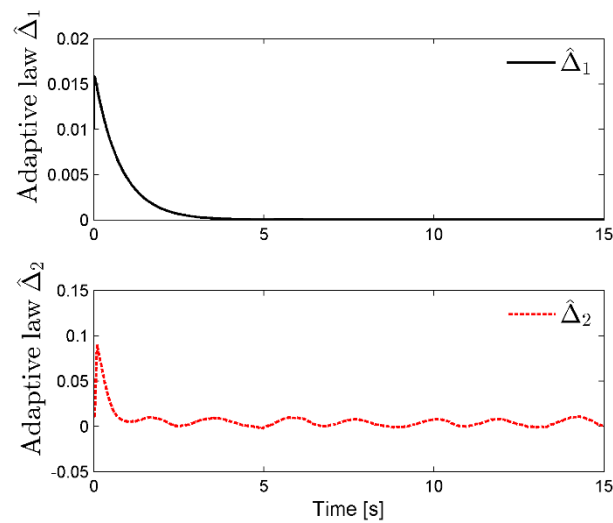


Figure 6. Trajectories of adaptive law $\hat{\Delta}_i$ ($i = 1, 2$).

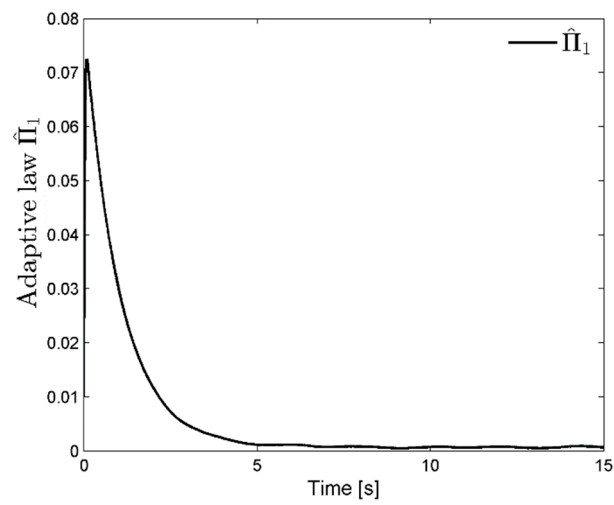


Figure 7. Trajectory of adaptive law $\hat{\Pi}_1$.

Considering Example 2, the simulation results are given in Figures 8–13.

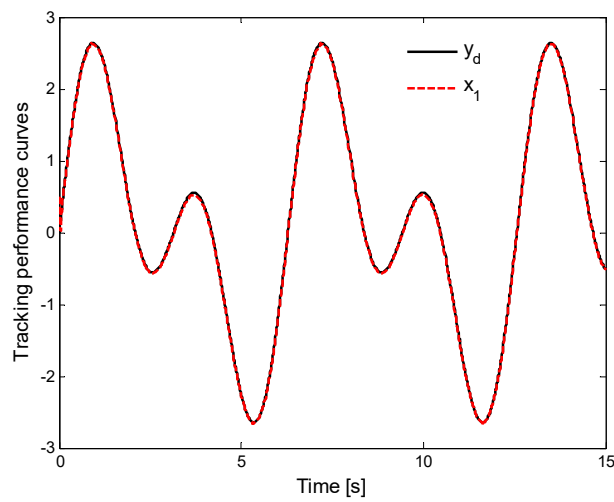


Figure 8. Trajectories of system output $x_1(t)$ and desired signal y_d .

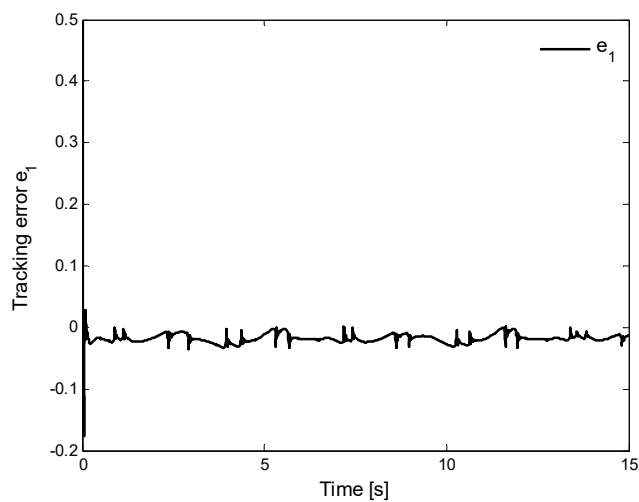


Figure 9. Trajectory of tracking error $e_1(t)$.

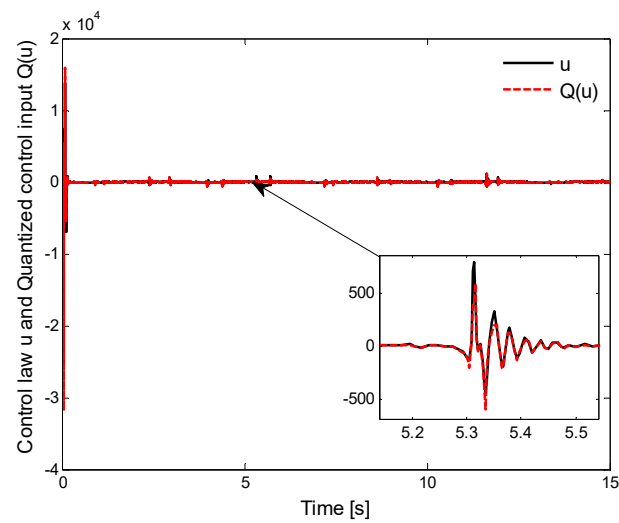


Figure 10. Trajectories of control law $u(t)$ and quantized control input $Q(u)$.

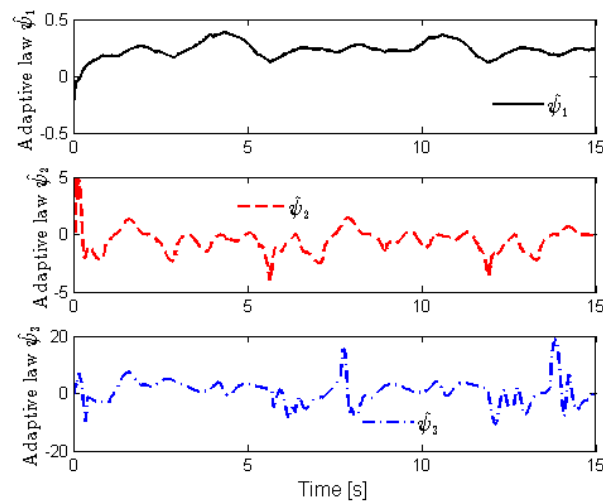


Figure 11. Trajectories of adaptive law $\hat{\psi}_i$ ($i = 1, 2, 3$).

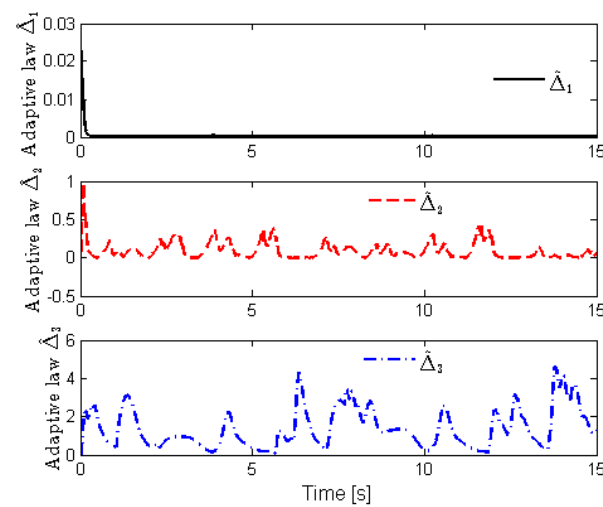


Figure 12. Trajectories of adaptive law $\hat{\Delta}_i$ ($i = 1, 2, 3$).

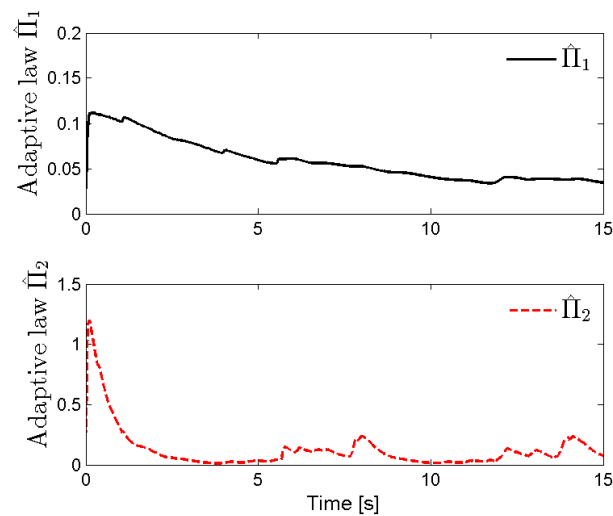


Figure 13. Trajectories of adaptive law $\hat{\Pi}_i$ ($i = 1, 2$).

The trajectories of the tracking performance and the tracking error are shown in Figures 8 and 9, respectively. It can be seen that the designed control law could achieve good tracking performance, and that the tracking error could converge on the small neighborhood of the origin. This also verified the validity of the theoretical analysis from another perspective. Figure 10 shows the trajectories of the control law and quantized control input. Similarly, there was a trade-off between a high control gain and tracking error. In addition, Figures 11–13 show the trajectories of adaptive laws $\hat{\psi}_i$, $\hat{\Delta}_i$ and $\hat{\Pi}_i$, respectively.

Remark 5. From the two examples, it can be seen that the desired tracking control could be achieved using the designed control law. Although external disturbances and input quantization were considered, better tracking performance was obtained in this paper. From the figures of the two examples, it can be seen that the boundedness of all signals of the considered system were maintained and the tracking error could converge on the small neighborhood of the origin. Meanwhile, we should pay attention to the reasonable trade-off between a good tracking effect and control gain when selecting appropriate design parameters.

6. Conclusions

This paper discussed the adaptive tracking control problem of a type of strict-feedback fractional-order nonlinear system with input quantization and external disturbances. An adaptive dynamic surface control law was successfully designed. The validity of the designed control law was proved by theoretical analysis. Furthermore, two examples were given to verify the effectiveness of the theoretical analysis results. Simulation results showed that the given fractional-order systems could achieve good control performance. Moreover, all signals of these two given systems were bounded and the tracking error could converge on an arbitrary small neighborhood of the origin. Further research will focus on how to extend the presented control law to strict-feedback fractional-order systems with event-triggered inputs.

Author Contributions: Conceptualization, X.D.; formal analysis, F.Z., X.D., L.W.; funding acquisition, X.D., L.W.; investigation, F.Z., X.D. and L.W.; methodology, X.D. and L.W.; project administration, F.Z. and L.W.; resources, X.D. and L.W.; software, F.Z. and X.D.; supervision, L.W.; validation, X.D.; visualization, F.Z. and L.W.; writing—original draft, X.D.; writing—review and editing, F.Z., X.D. and L.W. All authors have read and agreed to the published version of the manuscript.

Funding: This work was partially supported by the Natural Science Research of Colleges and Universities of Anhui Province under grant KJ2020A0344 and KJ2020ZD39, and the Program for the Top Talents of Anhui Polytechnic University.

Institutional Review Board Statement: Not applicable.

Informed Consent Statement: Not applicable.

Data Availability Statement: Not applicable.

Conflicts of Interest: The authors declare no conflict of interest.

References

1. Luo, Y.; Chen, Y.; Pi, Y. Experimental study of fractional order proportional derivative controller synthesis for fractional order systems. *Mechatronics* **2011**, *21*, 204–214. [[CrossRef](#)]
2. Cao, J.; Ma, C.; Jiang, Z.; Liu, S. Nonlinear dynamic analysis of fractional order rub-impact rotor system. *Commun. Nonlinear Sci. Numer. Simul.* **2011**, *16*, 1443–1463. [[CrossRef](#)]
3. Lu, J. Chaotic dynamics and synchronization of fractional-order Arneodos systems. *Chaos Solitons Fractals* **2005**, *26*, 1125–1133. [[CrossRef](#)]
4. Izaguirre-Espinosa, C.; Munoz-Vazquez, A.J.; Sanchez-Orta, A.; Parra-Vega, V.; Fantoni, I. Fractional-order control for robust position/yaw tracking of quadrotors with experiments. *IEEE Trans. Control Syst. Technol.* **2019**, *27*, 1645–1650. [[CrossRef](#)]
5. Tang, Y.; Zhang, X.; Zhang, D.; Zhao, G.; Guan, X. Fractional order sliding mode controller design for antilock braking systems. *Neurocomputing* **2013**, *111*, 122–130. [[CrossRef](#)]
6. Zhe, Z.; Jing, Z. Asymptotic stabilization of general nonlinear fractional-order systems with multiple time delays. *Nonlinear Dyn.* **2020**, *102*, 605–619. [[CrossRef](#)]
7. Ha, S.; Chen, L.; Liu, H.; Zhang, S. Command filtered adaptive fuzzy control of fractional-order nonlinear systems. *Eur. J. Control* **2022**, *63*, 48–60. [[CrossRef](#)]
8. Li, Y.; Wei, M.; Tong, S. Event-triggered adaptive neural control for fractional-order nonlinear systems based on finite-time scheme. *IEEE Trans. Cybern.* **2022**, *52*, 9481–9489. [[CrossRef](#)]
9. Liu, H.; Cheng, L.; Tan, M.; Hou, Z. Exponential finite-time consensus of fractional-order multiagent systems. *IEEE Trans. Syst. Man Cybern. Syst.* **2020**, *50*, 1549–1558. [[CrossRef](#)]
10. Ni, J.; Liu, L.; Liu, C.; Hu, X. Fractional order fixed-time nonsingular terminal sliding mode synchronization and control of fractional order chaotic systems. *Nonlinear Dyn.* **2017**, *89*, 2065–2083. [[CrossRef](#)]
11. Liu, H.; Li, S.; Cao, J.; Li, G.; Alsaedi, A.; Alsaadi, F.E. Adaptive fuzzy prescribed performance controller design for a class of uncertain fractional-order nonlinear systems with external disturbances. *Neurocomputing* **2017**, *219*, 422–430. [[CrossRef](#)]
12. Liang, B.; Zheng, S.; Ahn, C.; Liu, F. Adaptive fuzzy control for fractional-order interconnected systems with unknown control directions. *IEEE Trans. Fuzzy Syst.* **2022**, *30*, 75–87. [[CrossRef](#)]
13. Liu, H.; Li, S.; Wang, H.; Sun, Y. Adaptive fuzzy control for a class of unknown fractional-order neural networks subject to input nonlinearities and dead-zones. *Inf. Sci.* **2018**, *454–455*, 30–45. [[CrossRef](#)]
14. Li, X.; Zhan, Y.; Tong, S. Adaptive neural network decentralized fault-tolerant control for nonlinear interconnected fractional-order systems. *Neurocomputing* **2022**, *488*, 14–22. [[CrossRef](#)]
15. Song, S.; Park, J.H.; Zhang, B.; Song, X.; Zhang, Z. Adaptive command filtered neuro-fuzzy control design for fractional-order nonlinear systems with unknown control directions and input quantization. *IEEE Trans. Syst. Man Cybern. Syst.* **2021**, *51*, 7238–7249. [[CrossRef](#)]
16. Peng, J.; Dubay, R. Adaptive fuzzy backstepping control for a class of uncertain nonlinear strict-feedback systems based on dynamic surface control approach. *Expert Syst. Appl.* **2019**, *120*, 239–252. [[CrossRef](#)]
17. Zhao, X.; Wang, X.; Zhang, S.; Zong, G. Adaptive neural backstepping control design for a class of nonsmooth nonlinear systems. *IEEE Trans. Syst. Man Cybern. Syst.* **2019**, *49*, 1820–1831. [[CrossRef](#)]
18. Koksal, N.; An, H.; Fidan, B. Backstepping-based adaptive control of a quadrotor UAV with guaranteed tracking performance. *ISA Trans.* **2020**, *105*, 98–110. [[CrossRef](#)]
19. Wang, C.; Lin, Y. Multivariable adaptive backstepping control: A norm estimation approach. *IEEE Trans. Autom. Control* **2012**, *57*, 989–995. [[CrossRef](#)]
20. Liu, H.; Pan, Y.; Cao, J.; Wang, H.; Zhou, Y. Adaptive neural network backstepping control of fractional-order nonlinear systems with actuator faults. *IEEE Trans. Neural Netw. Learn. Syst.* **2020**, *31*, 5166–5177. [[CrossRef](#)] [[PubMed](#)]
21. Song, S.; Zhang, B.; Xia, J.; Zhang, Z. Adaptive backstepping hybrid fuzzy sliding mode control for uncertain fractional-order nonlinear systems based on finite-time scheme. *IEEE Trans. Syst. Man Cybern. Syst.* **2020**, *50*, 1559–1569. [[CrossRef](#)]
22. Li, X.; Wen, C.; Zou, Y. Adaptive backstepping control for fractional-order nonlinear systems with external disturbance and uncertain parameters using smooth control. *IEEE Trans. Syst. Man Cybern. Syst.* **2021**, *51*, 7860–7869. [[CrossRef](#)]
23. Deng, X.; Zhang, C.; Ge, Y. Adaptive neural network dynamic surface control of uncertain strict-feedback nonlinear systems with unknown control direction and unknown actuator fault. *J. Frankl. Inst.* **2022**, *359*, 4054–4073. [[CrossRef](#)]
24. Edalati, L.; Sedigh, A.K.; Shooredeli, M.A.; Moarefianpour, A. Adaptive fuzzy dynamic surface control of nonlinear systems with input saturation and time-varying output constraints. *Mech. Syst. Signal Process.* **2018**, *100*, 311–329. [[CrossRef](#)]
25. Parsa, P.; Akbarzadeh-T, M.-R.; Baghbani, F. Command-filtered backstepping robust adaptive emotional control of strict-feedback nonlinear systems with mismatched uncertainties. *Inf. Sci.* **2021**, *579*, 434–453. [[CrossRef](#)]

26. Wang, H.; Kang, S.; Zhao, X.; Xu, N.; Li, T. Command filter-based adaptive neural control design for nonstrict-feedback nonlinear systems with multiple actuator constraints. *IEEE Trans. Cybern.* **2021**, *52*, 12561–12570. [[CrossRef](#)]
27. Ma, Z.; Ma, H. Adaptive fuzzy backstepping dynamic surface control of strict-feedback fractional-order uncertain nonlinear systems. *IEEE Trans. Fuzzy Syst.* **2020**, *28*, 122–133. [[CrossRef](#)]
28. Song, S.; Zhang, B.; Song, X.; Zhang, Z. Adaptive neuro-fuzzy backstepping dynamic surface control for uncertain fractional-order nonlinear systems. *Neurocomputing* **2019**, *360*, 172–184. [[CrossRef](#)]
29. Liu, H.; Pan, Y.; Cao, J. Composite learning adaptive dynamic surface control of fractional-order nonlinear systems. *IEEE Trans. Cybern.* **2020**, *50*, 2557–2567. [[CrossRef](#)]
30. Deng, X.; Wei, L. Adaptive neural network finite-time control of uncertain fractional-order systems with unknown dead-zone fault via command filter. *Fractal Fract.* **2022**, *6*, 494. [[CrossRef](#)]
31. Ha, S.; Chen, L.; Liu, H. Command filtered adaptive neural network synchronization control of fractional-order chaotic systems subject to unknown dead zones. *J. Frankl. Inst.* **2021**, *358*, 3376–3402. [[CrossRef](#)]
32. Shao, K.; Zheng, J.; Tang, R.; Li, X.; Man, Z.; Liang, B. Barrier function based adaptive sliding mode control for uncertain systems with input saturation. *IEEE/ASME Trans. Mechatron.* **2022**, 1–11. [[CrossRef](#)]
33. Yang, J.; Bu, X.; Yu, Q.; Zhu, F. Observer-based controller design for nonlinear semi-Markov switched system with external disturbance. *J. Frankl. Inst.* **2020**, *357*, 8435–8453. [[CrossRef](#)]
34. Xu, B.; Liang, Y.; Li, Y.; Hou, Z. Adaptive command filtered fixed-time control of nonlinear systems with input quantization. *Appl. Math. Comput.* **2022**, *427*, 127186. [[CrossRef](#)]
35. Tan, Y.; Xiong, M.; Du, D.; Fei, S. Observer-based robust control for fractional-order nonlinear uncertain systems with input saturation and measurement quantization. *Nonlinear Anal. Hybrid Syst.* **2019**, *34*, 45–57. [[CrossRef](#)]
36. Ma, H.; Liang, H.; Zhou, Q.; Ahn, C.K. Adaptive dynamic surface control design for uncertain nonlinear strict-feedback systems with unknown control direction and disturbances. *IEEE Trans. Syst. Man Cybern. Syst.* **2019**, *49*, 506–515. [[CrossRef](#)]
37. Lv, M.; de Schutter, B.; Shi, C.; Baldi, S. Logic-based distributed switching control for agents in power-chained form with multiple unknown control directions. *Automatica* **2022**, *137*, 110143. [[CrossRef](#)]
38. Sheng, D.; Wei, Y.; Cheng, S.; Shuai, J. Adaptive backstepping control for fractional order systems with input saturation. *J. Frankl. Inst.* **2017**, *354*, 2245–2268. [[CrossRef](#)]
39. Bigdeli, N.; Ziazi, H.A. Finite-time fractional-order adaptive intelligent backstepping sliding mode control of uncertain fractional-order chaotic systems. *J. Frankl. Inst.* **2017**, *354*, 160–183. [[CrossRef](#)]
40. Yu, Z.; Yang, Y.; Li, S.; Sun, J. Observer-based adaptive finite-time quantized tracking control of nonstrict-feedback nonlinear systems with asymmetric actuator saturation. *IEEE Trans. Syst. Man Cybern. Syst.* **2020**, *50*, 4545–4556. [[CrossRef](#)]
41. Liu, Y. Adaptive dynamic surface asymptotic tracking for a class of uncertain nonlinear systems. *Int. J. Robust Nonlinear Control* **2017**, *28*, 1233–1245. [[CrossRef](#)]
42. Wang, C.; Wen, C.; Lin, Y.; Wang, W. Decentralized adaptive tracking control for a class of interconnected nonlinear systems with input quantization. *Automatica* **2017**, *81*, 359–368. [[CrossRef](#)]
43. Huo, X.; Ma, L.; Zhao, X.; Zong, G. Observer-based fuzzy adaptive stabilization of uncertain switched stochastic nonlinear systems with input quantization. *J. Frankl. Inst.* **2019**, *356*, 1789–1809. [[CrossRef](#)]